The Influence of Tumor Stage and Metastasis on the Biodistribution of Gallium-67 Citrate in the Murine Lewis Lung Carcinoma Model

A. Kanclerz*, L. I. Wiebe, K. Luu, and E. E. Knaus

Faculty of Pharmacy and Pharmaceutical Sciences, University of Alberta and Department of Radiation Oncology, Cross Cancer Institute, Edmonton, Alberta

The biodistribution of i.v. administered [^{67}Ga]citrate was investigated in the Lewis lung carcinoma/male $B_6D_2F_1$ mouse model. Tumors were implanted intramuscularly (10^5 cells or 10^6 cells in suspension) into the thigh, or subcutaneously (10^7 cells or 2 mm^3 fragments) into the tail of recipient mice. Intramuscular tumors were allowed to grow for 16, 24, or 33 days; tail tumors developed for 2 wk (fragment implants) or 3 wk (10^7 cells in suspension) after which the primary tumor was amputated along with adjacent fragments of the tail tissue. Gamma camera scintigraphy and dissection/radiometric biodistribution studies indicated that: (a) tumors and metastases took up 5–6% of the injected dose/g except when large necrotic areas were present in the primary tumor; (b) blood levels of ^{67}Ga increased in all tumor-bearing animals, with up to tenfold increases in the i.m. tumor model at later stages of the growth; (c) hepatic uptake increased as a function of tumor size/age, and (d) all tissue:blood ratios declined as the neoplastic tissues progressed. The results are discussed with respect to tumor progression and metastatic disease.

J Nucl Med 29:1252–1258, 1988

The treatment of cancer is not successful in many instances because of failure to detect the primary tumor at a sufficiently early stage and the inability to treat subsequent metastases. Difficulties in locating metastases, in gaining access to them, and in developing a suitable therapeutic regimen are responsible for the lack of clinical results. Gamma scintigraphic studies using tumor-seeking radiopharmaceuticals can potentially assist the clinical oncologist in both of these areas (*1*). Gallium-67 (^{67}Ga) citrate is currently the radiotracer of choice for experimental and clinical scintigraphy in oncology despite its disadvantages which include cost, high radiation dose, low photon flux in the desired energy range, slow clearance through the liver and intestinal tract, and nonspecific uptake in absesses and in normal tissues damaged through trauma (*2–5*). Gallium-67 citrate has been used successfully in the clinic to image a number of cancers (*3,6*) including those in pulmonary (*7*) and lymphatic tissues (*8*). Its effectiveness as a screening agent is dependent upon the tumor type, and it has recently been postulated that the real clinical value of ^{67}Ga scintigraphy may lie not in the detection of tumors, but in the prediction of tumor malignancy (*9*). There are also numerous reports of ^{67}Ga use in tumor models (*10–12*) but there are no reports on ^{67}Ga biodistribution in experimental systems which have been allowed to develop over the full term of progression of the primary tumor and the development of spontaneous metastases which culminate in the animal's death.

Metastasis of the murine Lewis lung carcinoma (LLC) has now been studied by observing the biodistribution of [^{67}Ga]citrate at various stages of tumor growth. LLC has been used for many years in tumor biology research (*13*). Although this experimental model has been applied to screen various chemotherapeutic and diagnostic agents, there are no reports, to our knowledge, on the biodistribution of ^{67}Ga in this tumor. The influence of anatomic location, rate of growth, and size of the primary tumor on the formation of metastases in the lungs and in the lymphatic system, and on the response of normal and neoplastic tissues as reflected by [^{67}Ga]citrate uptake have been presented in a preliminary report (*14*) and are now reported in detail.

Received Sept. 28, 1987; revision accepted Feb. 12, 1988.

For reprints contact: *Present address: A. Kanclerz, Hamilton Regional Cancer Centre, 711 Concession St., Hamilton, Ontario, Canada, L8V 1C3.

MATERIALS AND METHODS

Inbred male $B_6D_2F_1$ mice (Charles River Laboratory, Wilmington, MA) weighing 20–25 g (8–10 wk old) at the time of implantation were used. The Lewis lung carcinoma (LLC) originated from the Institute of Cancer Research, London, England. LLC tumors were maintained in vivo by serial transplantation in mice at 10-day intervals using an intramuscular (i.m.) innoculation of freshly harvested, mechanically isolated tumor cells.

Experimental tumors were prepared by i.m. injection of isolated-cell suspension (25 μl of minimum essential medium containing 10^5 cells in one group and 10^6 cells in a second group) into the right thigh of recipient mice or by injecting 10^7 cells in 20 μl s.c. on the lateral side of the tail near the mid-point between its proximal and distal extremities. The viability of injected cells was >85% as determined by the Trypan blue exclusion test. Animals in a fourth experimental group were given implants of freshly-diced tumor tissue by s.c. insertion of the tumor fragment (~2 mm^3) into surgically-prepared pockets under the lateral surface of the tail (*15*).

Gallium-67 citrate was supplied by Mr. J. R. Scott of the Edmonton Radiopharmaceutical Centre. Animals bearing i.m. tumors for each innoculum-size group (10^5 and 10^6 cells) were randomly assigned to one of three sub-groups of six animals each: in each group four mice were used for the ^{67}Ga uptake and two were used for scintigraphic imaging, these studies being performed on Days 16, 24, and 33 after tumor transplantation. Studies on mice injected with 10^6 cells were performed only on Days 16 and 24, because there were no survivors after 30 days. Separate control groups of healthy animals were used on the same days, three for dissection to examine the quantitative biodistribution of ^{67}Ga and two for imaging. Animals with primary tail tumors (innoculum and fragment transplant groups) were studied 2–3 wk after transplantation. In a second group the primary tail tumors were removed by amputation of the tail after a 2–3 wk period, and further studies were undertaken after an additional 3–4 wk (6–7 wk after transplantation). In each case [^{67}Ga]citrate was injected into the lateral tail vein 48 hr before dissection or imaging at doses of 37 kBq and 3.7 MBq, respectively. On the predetermined day mice were killed by asphyxiation in carbon dioxide followed immediately by partial exsanguination through cardiac puncture. Tumors were surgically removed and their outer part separated from the inner, necrotic region in the case of intramuscular primary tumors. Primary tumors growing in the tail were difficult to separate from tail tissue and because of their small size, necrotic tissue was not evident. Pulmonary metastases and metastases in the regional lymph nodes were also excised, and the remaining and apparently healthy pulmonary tissue, liver, spleen, kidneys, and bone were dissected.

The amount of radioactivity in each sample was measured by gamma counting in a Beckman 8000 gamma well counter. Tissue:blood ratios, % of dose/organ and % of dose/g (% i.d./g) tissue were calculated for each tissue sample. Imaging was carried out using a Searle pho gamma camera/ADAC data system, on animals anesthesized with Ketamine and Xylazine. A pinhole collimator was used for imaging (100,000 counts per image) at an animal to crystal distance of 10 cm. Animals were killed after the final imaging for additional quantitative studies.

Statistical analysis of the data consisted of calculations of means and standard deviations in the sample groups and comparing the data to control data using the Student's t-test; $p \leq 0.05$ was considered significant.

RESULTS AND DISCUSSION

The primary tumors were palpable within 5–7 days after i.m. implantation, depending on the number of viable cells in the innoculum: the fewer cells injected, the longer the latency period between injection and tumor appearance (Fig. 1a). The tail tumors developed more slowly, with visible growth within 10–14 days in all successful transplants (Fig. 1c). The i.m. tumors were well defined, and their separation from surrounding tissues (Fig. 1b) for further experimental procedure did not pose technical problems even in the case of small tumors weighing as little as ~200 mg. The outer viable tissue was also separable from the inner, necrotic part. This allowed us to study ^{67}Ga distribution in viable and necrotic regions of tumors having different sizes. However, the proportion of viable to necrotic regions rapidly decreased with the tumor growth: 3 wk after transplantation, only a narrow outer rim of viable tissue was found. The s.c. tail tumors invade all histologic elements of the tail with the exception of the bone (Fig. 1d), and were difficult to isolate from normal tissues for ^{67}Ga biodistribution study.

Metastatic pulmonary tumors (Fig. 2) were macroscopically evident within 14 days in all animals. Due to the different anatomical sites of the primary tumors and different experimental procedures, it was possible to examine ^{67}Ga uptake not only in the primary tumors, but also in metastatic lesions of different stages (Fig. 3). Several vectors of metastatic spread were observed depending on the location of the primaries: i.m. LLC formed metastases in the iliac and inguinal lymph nodes, and neoplastic infiltration was more overt to the ipsilateral side of the tumors. LLC in the tail metastasized to the sacral, iliac, inguinal and paraaortic lymph nodes, and the nodes of both sides were equally involved in most of the experimental animals. Metastases in other organs were observed as well. The use of the tail implant model allowed us to follow development of metastases and to investigate ^{67}Ga biodistribution and its changes in secondary neoplastic disease without influence of any large primary tumor. Observation of full development of metastases in animals with i.m. tumors was not possible because large primary tumors, usually with concomitant massive pulmonary involvement, caused animals' death.

No active metastatic infiltration in liver, spleen, kidneys, and bones was observed during autopsy. This lack of visible metastases in organs was taken as evidence that metastatic disease was absent, although histologic examination was not undertaken.

FIGURE 1
Primary Lewis lung carcinoma in $B_6D_2F_1$ mice. a: Three weeks after transplantation of 10^5 viable cells. Tumors are growing intramuscularly in the right gastrocnemius muscle. b: Excised i.m. tumor showing spherical shape. Transplantation of mechanically isolated viable cells allowed us to perform experiments on biologically similar tumors of approximately the same volume. Distance between bars 1 cm. c: Two weeks after subcutaneous implantation in the tail. Amputation of the tumor with adjacent fragments of the healthy tissue was performed the same day. d: Transverse section of the tail tumor. Neoplastic tissue invades all histological elements of the tail with their subsequent destruction. Infiltration of the skin with ulceration is seen on the top surface of the tumor. Bone was excised prior to processing. Hematoxylin and eosin stain; ×7.

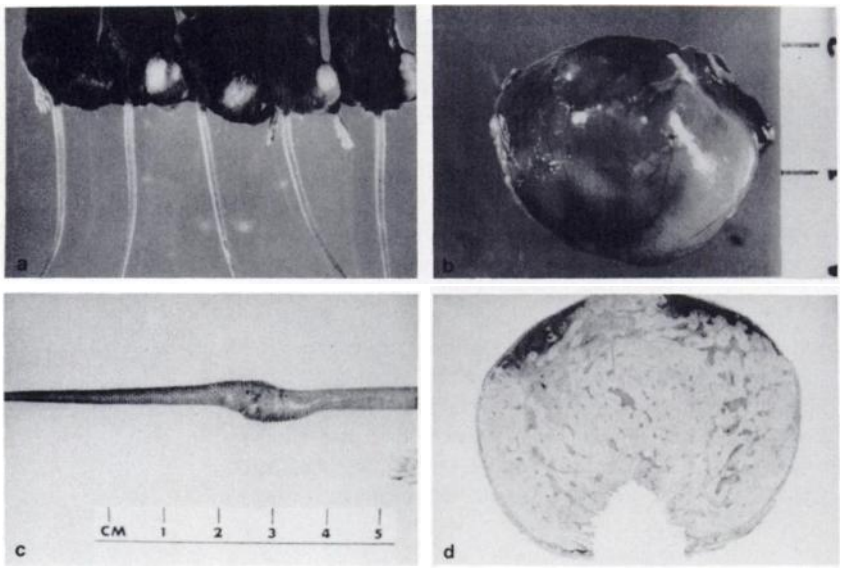

The pattern of ^{67}Ga biodistribution in the three LLC transplantation modes used (i.m. cells, s.c. cells and tumor implants) was complex, but several features appeared to be directly related to primary tumor progression and development of metastases (Table 1). Blood levels 48 hr after i.v. injection of [^{67}Ga]citrate were much lower in the $B_6D_2F_1$ strain (0.2 ± 0.04% i.d./g) than in other murine strains; recently reported % i.d/g values for murine tumor models include 2.26 ± 0.06 for the ddY Ehrlich model (*16*), 0.6 ± 0.1 for the BALB/c EMT-6 model (*17*) and 1.75 ± 0.28 for the C3H/HEN-mammary adenocarcinoma model (*18*). These differences could reflect specific activity (*5*) or commercial source (*19*) of ^{67}Ga, although in at least one case (*17*) the commercial source and specific activity were virtually identical to the ^{67}Ga used here. In the slowly growing tail transplant group, blood levels were not significantly different from control blood levels, but in other groups large increases were seen (Table 1). In the tail s.c. cells transplantation group, blood levels were double the control values with little change over a 3-wk period. In the i.m. group, there was a qualitative relationship between blood level and tumor mass, with ^{67}Ga levels about ten times higher in the animals with the largest primary/metastatic tumor mass (24 days after transplantation of 10^6 cells). No attempt was made to precisely determine total tumor burden, but the estimated values based on dissected tumor tissue ranged

FIGURE 2
Pulmonary metastases of Lewis lung carcinoma. a: Separate lobe of excised fresh lungs showing extensive metastatic involvement. Metastases (arrows) of different size are visible on the surface. Distance between bars 1 mm. b: Metastatic nodules on the lung surface from a. Note haemorrhagic foci (arrow) in the lesion. Distance between bars 1 mm. c: Macrophotograph of the lungs with advanced metastatic disease. Multiple metastases infiltrate the whole volume of the organ with massive destruction of the healthy tissue. Hematoxylin and eosin stain; ×4.5. d: Higher-magnification photomicrograph of a selected area from c; ×64.

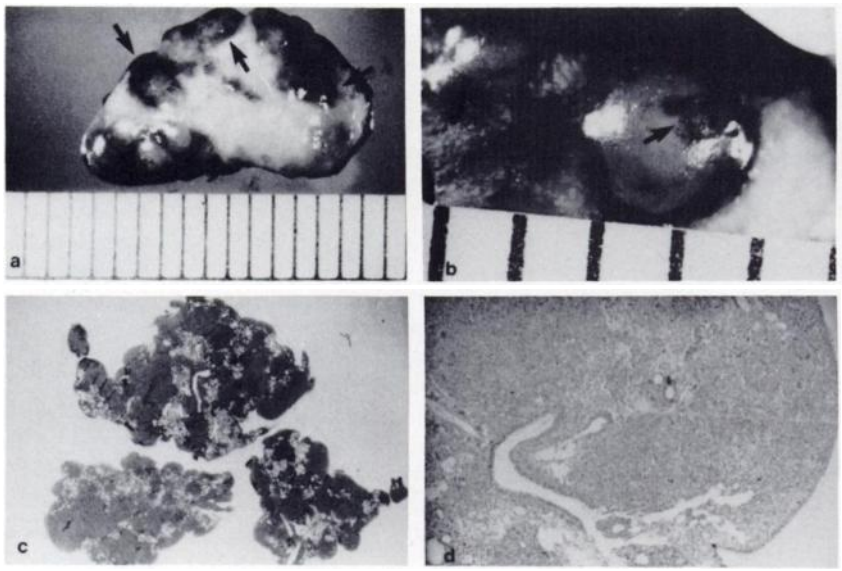

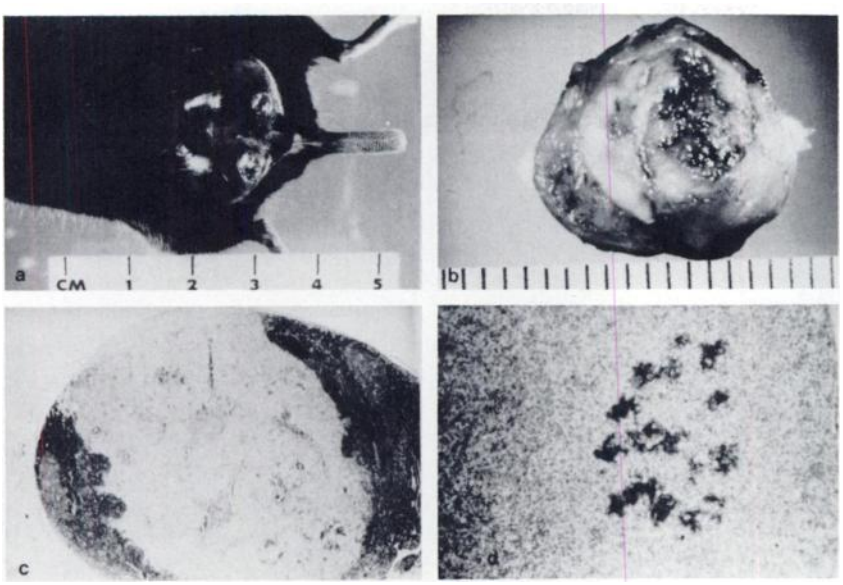

FIGURE 3
Lymph node metastases in the tail implant model. a: Large bilateral sacral metastases three weeks after tumor surgery. b: Excised sacral metastasis. Note big augmentation of the volume due to extensive metastatic infiltration. Necrosis is seen in the center. Distance between bars 1 mm. c: Lewis lung carcinoma cells invading into parenchyma of a lymph node. Fragments of the normal lymphatic tissue are seen on both sides of the macrophotograph. Hematoxylin and eosin stain; ×20. d: Complete destruction of the lymph node. Small fragments of the residual lymphatic tissue are seen in the center of the photomicrograph. Hematoxylin and eosin stain; ×51.

from 1% of body weight at 14 days after 10^5 cells i.m., to more than 10% 24 days after transplantation of 10^6 cells. No animals survived more than 28–30 days after i.m. inoculation with 10^6 cells. It appears that growth of the primary tumor is mainly responsible for the elevated blood levels, since there were no changes over the 3–4 wk period between amputation of the primary tail tumors and the final measurement 6 wk after transplantation. That is, when compared to the i.m. tumor data, the absence of a large tumor burden in the tail tumor models appears to account for the absence of large elevations of ^{67}Ga blood levels in the latter group.

Elevation of ^{67}Ga concentrations in apparently healthy pulmonary tissue also occurred (Table 1). These data may reflect the presence of ^{67}Ga-avid tumor microfoci or simply the presence of residual blood which has higher ^{67}Ga concentrations. Gallium-67 concentrations in pulmonary metastases were proportional to ^{67}Ga in healthy lung tissue; this and the presence of hemorrhagic regions in both apparently-cancer-free and metastatic tissue (Fig. 2b) are supportive in part of a blood-pooling mechanism. In three groups (10^6 i.m. 24 days; 10^7 s.c. 21 days and 42 days after transplantation) pervasive metastatic tissue either precluded separation of healthy lung from neoplastic tissue or killed animals prematurely. In the tail s.c. cells transplantation group, the rapid development of metastases was taken as evidence that this transplantation method produces "ex-

TABLE 1
Uptake of ^{67}Ga in Primary Tumors, Metastases and Healthy Tissues in Various Models of the LLC in $B_6D_2F_1$ Mice

		Percent of injected ^{67}Ga per g tissue (mean ± s.d.; n = 3)				
Animal model	Body weight (g) mean ± s.d.	Blood	Primary tumor	Pulmonary metastases	Mediastinal lymphatic tissue	Lung
control	25.7 ± 0.6	0.20 ± 0.05	—	—	1.38 ± 0.75	1.09 ± 0.22
10^5 i.m. 16d	24.3 ± 2.3	0.46 ± 0.05§	2.51 ± 0.53	2.8*	2.53 ± 0.53	1.52 ± 0.10§
10^5 i.m. 24d	26.2 ± 1.4	0.48 ± 0.03§	2.17 ± 0.32	2.91 ± 0.73	2.21 ± 0.39	1.36 ± 0.11§
10^5 i.m. 33d	26.7 ± 1.5	0.75 ± 0.09§	1.32 ± 1.19	2.91 ± 0.73	2.17 ± 0.34	1.74*
10^6 i.m. 16d	26.9 ± 0.9	1.32 ± 0.23§	5.25 ± 2.16	6.74 ± 2.19	5.20 ± 1.59§	4.23 ± 1.27§
10^6 i.m. 24d	26.7 ± 1.2	2.22 ± 0.16§	1.99 ± 0.39	†	4.51 ± 2.42	†
s.c. fragment 14d	26.0 ± 1.2	0.27 ± 0.03	2.07 ± 0.47	—	1.30 ± 0.73	0.96 ± 0.22
s.c. fragment 42d	27.6 ± 0.5	0.26 ± 0.03	—	1.34 ± 0.09	0.96 ± 0.30	0.84 ± 0.09
10^7 s.c. 21d	27.4 ± 1.2	0.51 ± 0.05§	3.21 ± 0.40	—	3.06 ± 0.97	1.58 ± 0.23§
10^7 s.c. 42d	28.6 ± 0.8	0.51 ± 0.09§	—	2.3‡	3.68 ± 1.92	1.35 ± 0.20

— Not measured or not applicable.
* Single animal.
† Advanced metastatic disease; tissues not separable.
‡ Single survivor with visible metastases.
§ Significantly different from control ($p < 0.05$).

perimental" metastases as well as "spontaneous" metastases. Indeed, the LLC may be injected directly into the tail vein to induce experimental pulmonary metastases (*20*). Because of the differences between experimental and spontaneous models of metastases, and because of primary tumor growth irregularities, the tail s.c. cells transplantation method was considered inappropriate for radiotracer biodistribution studies (15).

Quantitative uptake of ^{67}Ga in the lymphatic system was best demonstrated in mediastinal lymphatic tissue (Table 1). Although regional differences in lymph node enlargement were evident among the various transplantation groups, lymphatic tissue also had higher levels of ^{67}Ga when other tissues showed increases.

The amount of ^{67}Ga in the primary tumors ranged from 1.3–5.25% i.d./g, the highest concentrations being present in the "young" (10^6 cells in innoculum; 16 days after transplantation) but large i.m. tumors and lowest in older, moderately large (10^5 cells in innoculum; 33 days after transplantation) tumors. All i.m. tumors had visible nonviable (necrotic) central regions; the larger tumors had very thin layers of viable tissue at the surface of the tumor and consequently had low tumor uptake values. In "younger" tumors, the viable tumor accumulated more ^{67}Ga than the necrotic areas (3.4 ± 1.5% i.d./g versus 1.5 ± 0.5% i.d./g), but these differences became less apparent as the tumor size increased (1.4 ± 0.1% i.d./g versus 1.3 ± 0.4% i.d./g); this observation may in part reflect a procedural artifact because in many tumors it was difficult to adequately dissect the thin layer of viable tissue from the nonviable center. Tumor size/age and regional necrosis have been shown to affect ^{67}Ga uptake by implanted tumors in other tumor models (*21*). Tumor growth kinetics has been reported to affect ^{67}Ga uptake by the primary tumor (*22*), but this was not evident with LLC in these studies: the fastest tumor growth was observed in the groups injected i.m. with 10^6 cells and the slowest in the tail implant group.

Tumor:blood and tissue:blood ratios reflect relative radiotracer concentrations which give rise to contrast in scintigraphy. Although the concentrations of ^{67}Ga (% i.d./g) increased in liver, concentrations in lungs, spleen, kidney, and bone remained constant or decreased slightly as the neoplastic disease progressed. However, liver:blood ratios, as well as other tissue:blood ratios dropped dramatically in animals with advanced neoplastic disease (Fig. 4). In liver, for example, normal $B_6D_2F_1$ mice had 3.8 ± 0.8% i.d./organ compared to 15.5 ± 5.0% i.d/organ in the animals 24 days after transplantation of 10^6 cells, in spite of a 30–35% decrease in liver size; the liver:blood ratios declined from 13.4 ± 1.5 to 6.7 ± 1.0 at the same time. The tumor:blood ratios were relatively constant at ~5–6 in young primary i.m. tumors and in pulmonary metastases, but these ratios declined to ~2 in the oldest primaries (33 days after transplantation). The viable tumor areas had tumor:blood ratios of ~8 and necrotic tumors had ratios of ~3.4. In the 33 day i.m. tumor (10^5 cell innoculum), there were no differences between inner (necrotic) and outer regions, probably an artifactual consequence to difficulties in cleanly isolating the thin shell of viable outer tissue.

The scintigrams (Fig. 5) demonstrate clearly that

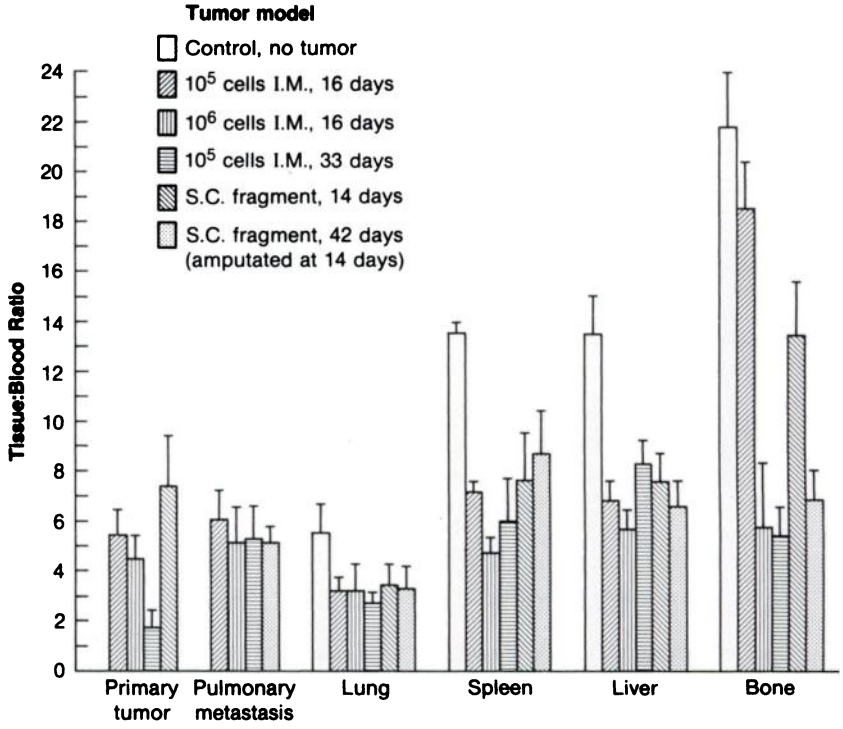

FIGURE 4
Tissue:blood ratios in the LLC/$B_6D_2F_1$ model, showing the effects of transplantation mode and growth interval on relative biodistributions of ^{67}Ga 48 hr after i.v. injection of [^{67}Ga] citrate.

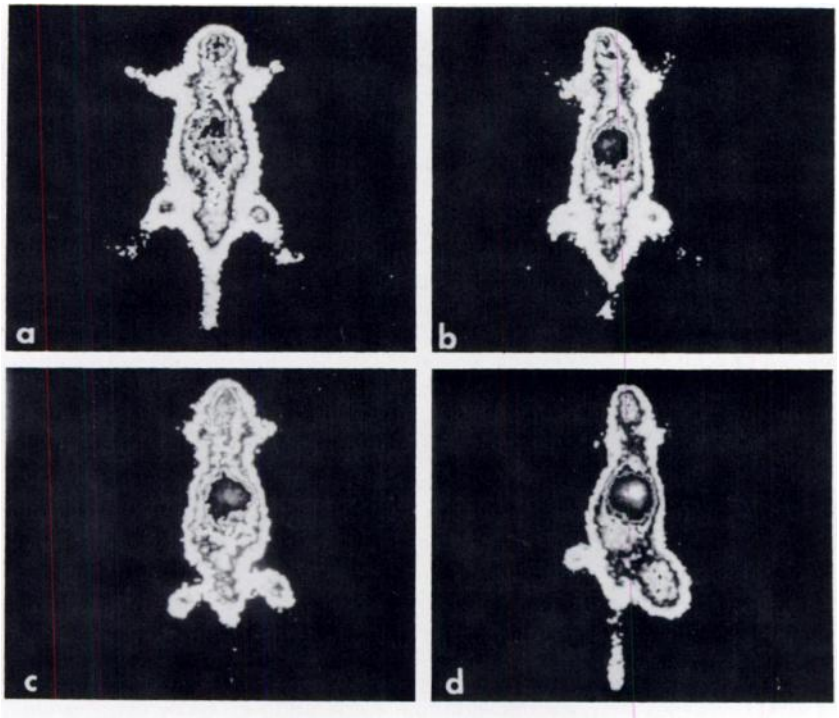

FIGURE 5
Scintigrams of $B_6D_2F_1$ mice 48 hr after i.v. injection of [^{67}Ga]citrate. a: Normal mouse. b: 42 days after transplantation of 10^7 tumor cells into the tail and 14 days after removal of the primary tumor. c: 10^5 cells i.m. 16 days after transplantation. d: 10^6 cells i.m. 32 days after transplantation.

although primary i.m. tumors as small as 200 mg and tail tumors as small as 20 mg are scintigraphically visualized 48 hr after i.v. injection of ^{67}Ga, the scintigraphic detection of enlarged lymph nodes (up to 5 mg) and multiple pulmonary metastases (5–20 mg each) is compromised by the combined effects of elevated blood levels, similar tissue:blood ratios for bone and viscera, and the relatively large mass and increased uptake of the underlying (radioactive) liver. Increased radioactivity seen in the region of the lungs and liver as a function of progression of neoplastic disease reflects growth of pulmonary metastases only in part. The higher uptake of ^{67}Ga by the livers of these animals (Fig. 5) precludes interpretation of the scintigrams in terms of pulmonary metastases only. It has been shown that the relative position of lungs and liver is such that hepatic and pulmonary radioactivity is difficult to differentiate in murine scintigrams (*23*).

The i.m. and tail transplantation methods produce spontaneous metastases. Implanted tail tumors grow slowly because of poor vascularity, large amounts of connective tissue and physical constraints. Tail tumors take up about the same amount (% i.d./g) of ^{67}Ga as is taken up by i.m. primary tumors. The most important difference between the i.m. and s.c. tail transplantation methods is that the altered ^{67}Ga biodistribution observed in blood, bone and viscera of the i.m. model was not seen in the tail tumor model. A ^{67}Ga biodistribution effect in non-neoplastic tissues is not in agreement with an earlier report of ^{67}Ga biodistribution in other tumor models (*21*). However, the earlier investigation did not report on the respective tumor models over the full period of tumor growth and formation of metastases. A previous report of the nonspecific decrease in ^{67}Ga uptake by bone attributed the effect to host age (*24*). In those studies, however, blood levels remained virtually constant over a 51-day period, whereas blood levels increased ~tenfold over a 33-day period in our experiments; this suggests that different or additional factors besides passive absorption by bone are responsible for the changes reported here.

The LLC/$B_6D_2F_1$ tumor model produces varying ^{67}Ga biodistribution data depending on the method of transplantation, anatomical site of the growing tumor and the stage of neoplastic disease. The i.m. transplantation method does induce tumor size-related changes in ^{67}Ga biodistribution. It is therefore important to recognize that similar tumor-related changes may also occur with other tumor models. The possibility of altered responses should be kept in mind when screening radiotracer uptake in the LLC/$B_6D_2F_1$ model or when using ^{67}Ga or other radiotracers to characterize any experimental tumor models.

ACKNOWLEDGMENTS

This work was supported by grants from the Medical Research Council of Canada and the Alberta Cancer Board. The assistance provided through the Job Development Program, Canada Employment Centre (Dr. Luu) is gratefully acknowledged. The authors thank Dr. J. R. Mercer for his assistance with some of the experimental work and for preparing the scintigrams, Mr. Willard Dylke for transplanting tumors, and Ms. Carolyn Johnson for her patience in typing the manuscript.

REFERENCES

1. Diehl V, Schell-Frederick E. Nuclear oncology: current role and future direction. In: Winkler C, ed. *Nuclear medicine in clinical oncology.* Heidelberg: Springer-Verlag, 1986:3–9.
2. Tsan M-F, Scheffel U. Mechanism of gallium-67 accumulation in tumors. *J Nucl Med* 1986; 27:1215–1219.
3. Johnston GS. Clinical applications of gallium in oncology. *Int J Nucl Med Biol* 1981; 8:249–255.
4. Larson SM. Mechanisms of localization of gallium-67 in tumors. *Semin Nucl Med* 1978; 8:193–203.
5. Hayes RL. The medical use of gallium radionuclides: a brief history with some comments. *Semin Nucl Med* 1978; 8:183–191.
6. Bekerman C, Hoffer PB, Bitran JD. The role of gallium-67 in the clinical evaluation of cancer. *Semin Nucl Med* 1984; 14:296–323.
7. Schümichen C. Clinical aspects of detection and imaging of lung tumors. In: Winkler C, ed. *Nuclear medicine in clinical oncology.* Heidelberg: Springer-Verlag, 1986: 74–79.
8. Hör G, Munz DL, Brandhorst I, et al. Scintigraphy of lymphokinetics and lymphatic neoplasia. In: Winkler C, ed. *Nuclear medicine in clinical oncology.* Heidelberg: Springer-Verlag, 1986: 94–107.
9. Lentle BC, Scott JR, Schmidt RP, et al. The clinical value of direct tumor scintigraphy: a new hypothesis. *J Nucl Med* 1985; 26:1215–1216.
10. Haynie TP, Konikowski T, Glenn HJ. Experimental models for the evaluation of radioactive tumor-localizing agents. *Semin Nucl Med* 1976; 6:347–69.
11. Konikowski T, Glenn HJ, Haynie TP. Kinetics of ^{67}Ga compounds in brain sarcomas and kidneys of mice. *J Nucl Med* 1973; 14:164–171.
12. Wiebe LI. Small animal oncological models for screening diagnostic radiotracers. In: Lambrecht RM, Eckleman WC, eds. *Animal models in radiotracer design.* New York: Springer-Verlag, 1983: 107–148.
13. Steel GG. Growth kinetics of tumors. Oxford: Clarendon Press, 1975.
14. Wiebe LI, Kanclerz A, Luu K, et al. A mouse tumor model for screening radiotracer uptake into primary neoplasms and metastatic disease. In: Kristensen K, Nørbygaard E, eds. *Safety and efficacy of radiopharmaceuticals.* Dordrecht: Martinus Nijhoff, 1987: 115–125.
15. Kanclerz A, Chapman JD. The effectiveness of cisplatinum, cyclophosphamide and mephalan in treating disseminated tumor cells in mice. *Clin Exp Metast* 1987; 5:199–211.
16. Sasaki T, Kojima S. ^{67}Ga uptake and heparan sulfate content of Ehrlich solid tumor in mice. *Eur J Nucl Med* 1986; 12:182–186.
17. Gati LJ, Wiebe LI, Tse JW, et al. Comparative studies of radiocitrates in oncological models. I. ^{99m}Tc citrate and ^{67}Ga citrate uptake by EMT-6 tumors in mice. *Nucl Med Biol* 1986; 13:253–255.
18. Saha GB, Boyd CM. Tissue distribution of [^{67}Ga] citrate and $^{111}InCl_3$ in mouse with adenocarcinoma. *Int J Nucl Med Biol* 1983; 10:223–225.
19. Davis MA, Rebekah A, Taube RA, et al. Comparison of the biologic distribution of three commercially available Ga-67 citrate preparations in normal and diseased rats [Abstract]. *J Nucl Med* 1977; 18:617.
20. Carpentier Y. Extension tumorale et métastatique du carcinome pulmonaire de Lewis en fonction de la voie d'administration. Application à l'étude pharmacologique d'un produit. *Soc Biol de Reims* 1973; 1021–1028.
21. Hayes RL, Byrd BL, Carlton JE, et al. Factors affecting the localization of ^{67}Ga in animal tumors [Abstract]. *J Nucl Med* 1970; 11:324.
22. Bichel P, Hansen HH. The incorporation of ^{67}Ga in normal and malignant cells and its dependence on growth rate. *Br J Radiol* 1972; 45:182–184.
23. Shysh A, Eu SM, Noujaim AA, et al. Radioimmunodetection of murine mammary adenocarcinoma (TA3/Ha) lung and liver metastases with radioiodinated PNA. *Int J Cancer* 1985; 35:113–119.
24. Sephton RG, Hodgson GS, DeAbrew S, et al. Ga-67 and Fe-59 distributions in mice. *J Nucl Med* 1978; 19:930–935.